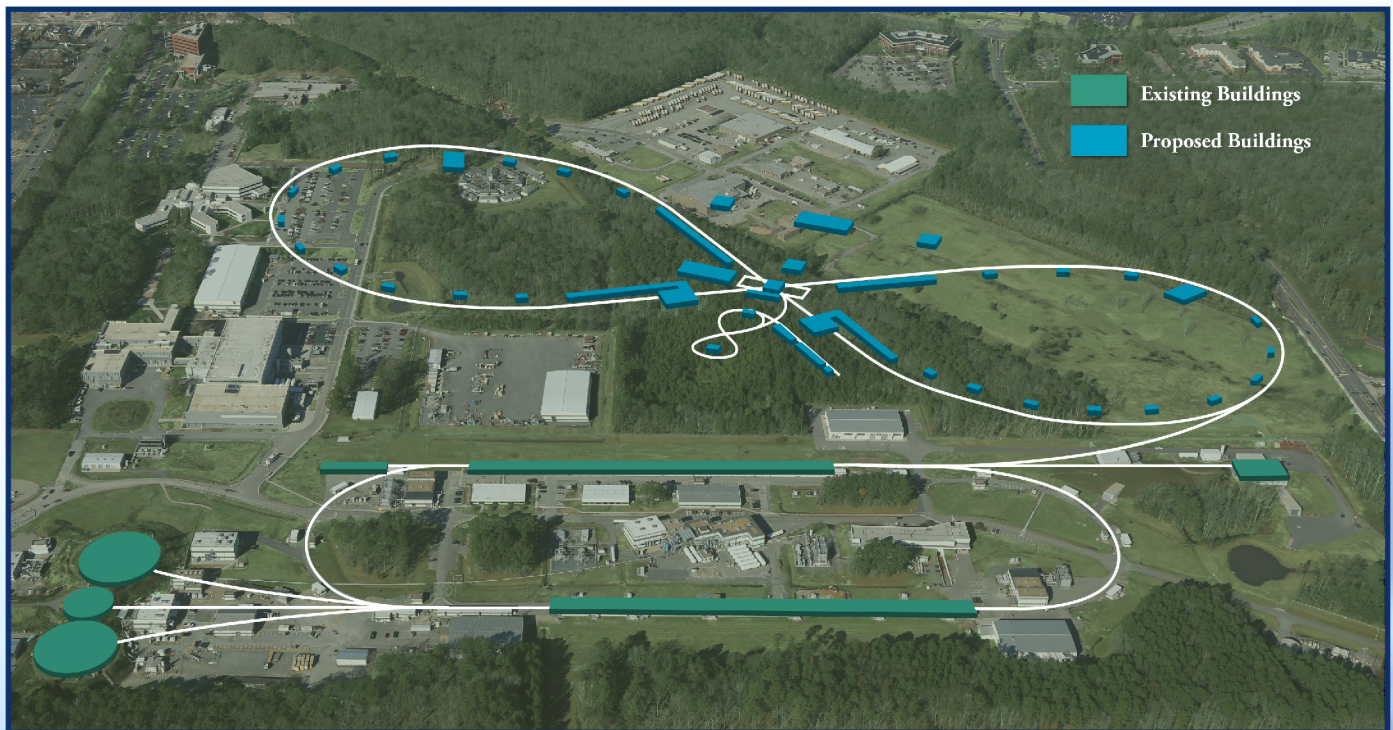


# Jefferson Lab Electron-Ion Collider (JLEIC):

An Introduction to the Interaction Region and Detector Design

*Authored by the JLEIC Detector and Interaction Region Study Group*



Jefferson Lab Electron-Ion Collider is a proposed realization of the Electron-Ion Collider (EIC) [1]. The EIC has been chosen as the highest priority new construction for Nuclear Physics in the US [2]. We discuss the main drivers for design of the JLEIC interaction region and the detectors, and the layout that was developed in response to these drivers.

[1] A. Accardi et al., *Electron Ion Collider: The Next QCD Frontier - Understanding the glue that binds us all*, JLAB-PHY-12-1652, 2012.

[2] A. Aprehmanian et al., *Reaching for the horizon: The 2015 long range plan for nuclear science*, 2015.

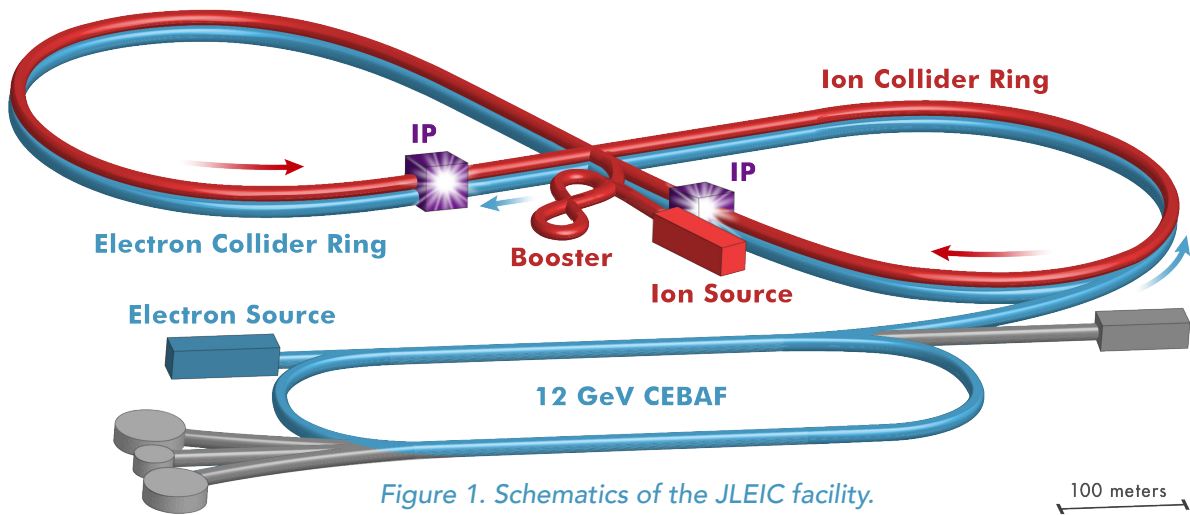


Figure 1. Schematics of the JLEIC facility.

## Jefferson Lab Electron-Ion Collider

The Jefferson Lab proposal for the Electron-Ion Collider (JLEIC) builds on the existing CEBAF accelerator as a full-energy injector and adds a new ion complex to achieve collisions of electrons of energies up to 10 GeV with protons of energies up to 100 GeV, as well as ions of energies of  $100 \times (Z/A)$  GeV/nucleon [3]. The JLEIC design aims for high luminosities of  $10^{34} \text{ cm}^{-2}\text{s}^{-1}$  and high polarization. The electron and ion rings are stacked in an innovative figure-8 design that allows proton and light-ion polarization in excess of 70%. The two interaction points (IP) sit in the straight sections relatively close to the exit of the ion bend arc and far from the exit of the electron bend arc in order to

avoid the ion related beam-gas background and synchrotron radiation background respectively.

[3] S. Abeyratne et al., MEIC Design Summary, JLAB-ACP-15-2036, 2015.

## Physics Processes at the Electron Ion Collider and Acceptance requirements

The basic physics process at the Electron-Ion Collider (EIC) is Deep Inelastic Scattering (DIS), which is represented in Fig. 2.

In the figure, an ion, composed of nucleons, in turn composed of partons (quarks and gluons), moves to the right and collides with an electron moving to the left. The electron collides with a parton within the ion in a hard collision.

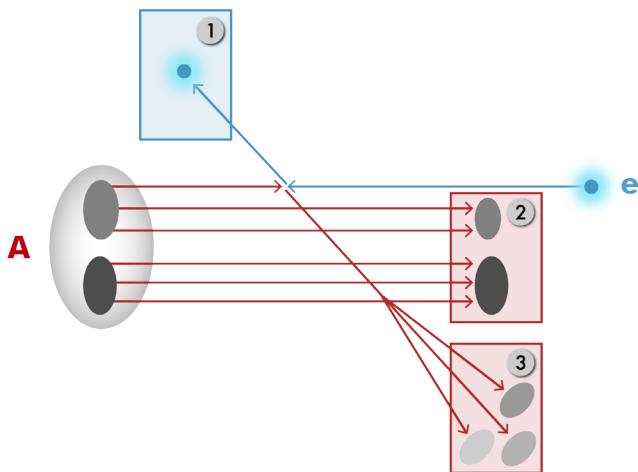


Figure 2: Classification of the final-state particles of a DIS process at the EIC: scattered electron (1), the particles associated with the initial state ion (2), and the struck parton (3).

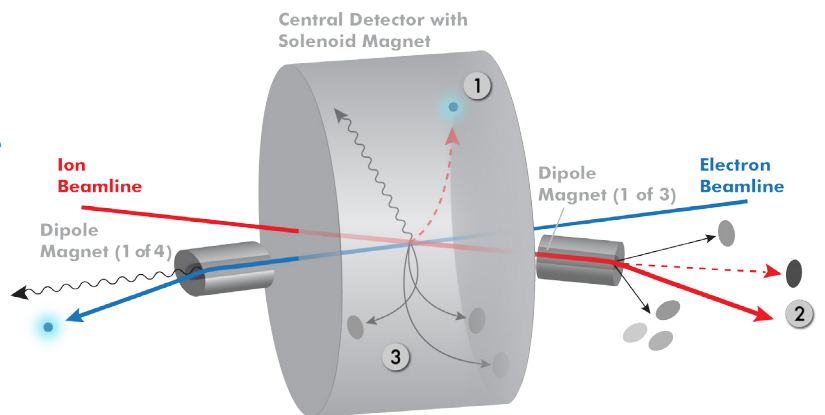


Figure 3: JLEIC IR and detector concept illustrating the crossing angle between the electron and ion beams and the dipole magnets downstream of the Central Detector. f

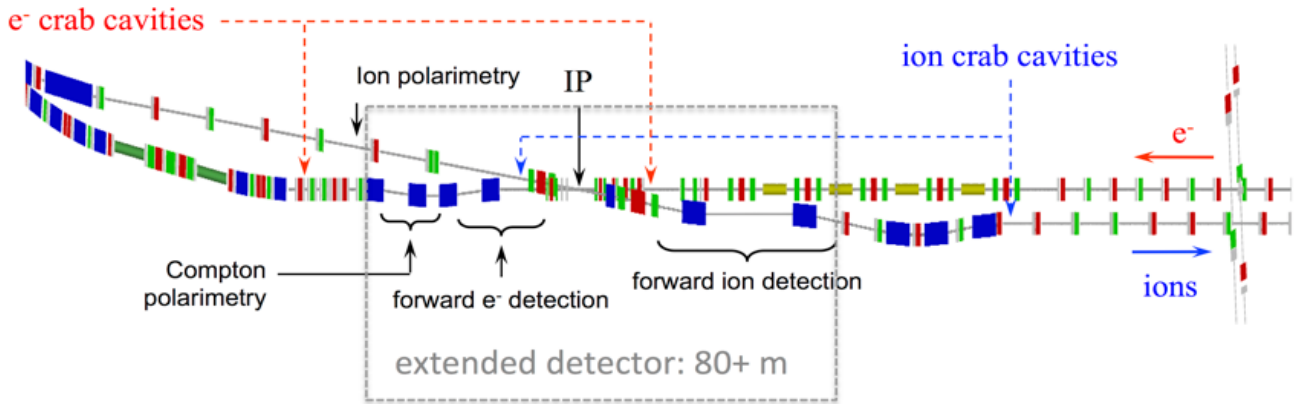


Figure 4: JLEIC design and extended detector: Accelerator elements in the IR and downstream the electron and ion beams are shown. The dark blue elements are dipoles where as red and green elements are beam quadrupoles. The Central Detector is placed asymmetrically around the interaction point (IP). Forward electron (ion) detectors will be installed in the downstream electron (ion) area. The locations for the electron (labeled as Compton polarimetry) and ion polarimetry are also shown.

We can, qualitatively, define three classes of particles in the final state.

1. The scattered electron
2. Particles associated with the initial state ion.
3. Particles associated with the struck parton.

The aim of the EIC is the investigation of the QCD structure of hadrons including ions and nucleons. All three types of final state particles carry information about the ion. Therefore it is essential that the interaction region (IR) and the detector at the EIC are designed so that all three types of particles are measured at as close to 100% acceptance as possible and with the necessary resolutions. We define the concept of a total acceptance detector as one that achieves close to 100% acceptance for all three types of particles.

## Total Acceptance Detector

The difficulty in achieving good acceptance in the forward regions at a collider has to do with the accelerator elements needed to deliver the colliding beams.

To first order, the luminosity at the IP is inversely proportional to the distance between the last upstream and first downstream final focus quadrupoles (FFQs). Thus, the statistical uncertainty of measurements at the Central Detector scales as  $\sqrt{\text{distance}}$ . On the other hand, the closer the beam elements are to

the IP, the more they obstruct the acceptance at shallow angles with respect to the beam axis and restrict the acceptance for forward particles. Also, the solenoidal field used in the central detector region to measure the high  $P_t$  particles in the central detector is not effective in determining the momenta of particles moving parallel to the beam direction, and additional fields are needed.

The JLEIC IR and detector concept, shown in Fig. 3 is designed to overcome the measurement difficulties posed by the beam elements. The ion and electron beams cross at a relatively large angle of 50mrad at the IP. High luminosity is preserved through the use of crab cavities. This angle moves the ion beam away from the electron beam elements and makes room for dipoles located just downstream of the central detector area. The dipoles serve two purposes. First, they shape the ion beam orbit so that there is 1 m distance between the two beams 30 m away from the IP, making room for detectors. Second, the dipole systems allow momentum analysis of the particles with small transverse momentum with respect to the beams. The particles with large transverse momenta are analyzed using the solenoidal field in the central detector.

The JLEIC design and the extended detector are shown in Fig. 4. The central detector is about 12.5 m in length and is a compromise

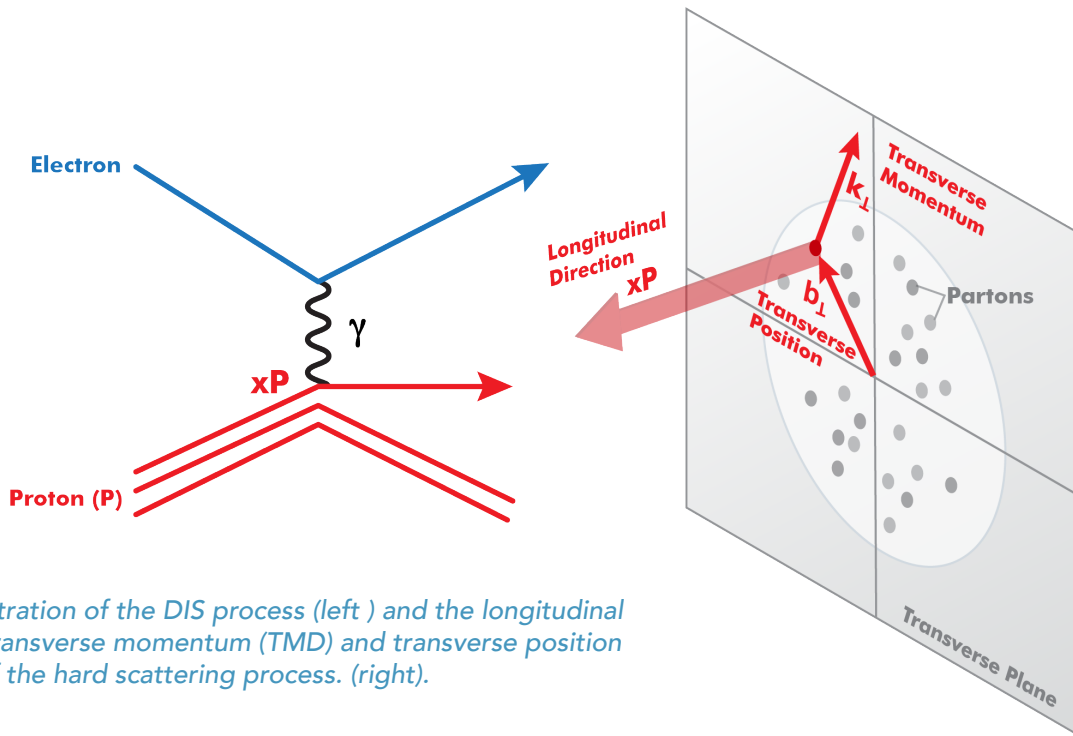


Figure 5: Illustration of the DIS process (left) and the longitudinal momentum, transverse momentum (TMD) and transverse position information of the hard scattering process. (right).

between luminosity and space considerations for the detectors.

The detection regions in the electron and ion beam directions extend 30-40m in either direction from the central detector. In the next section, the requirements and design for the central detector, the far-forward hadron detector and far-forward electron detector regions are discussed in turn.

## DETECTOR REGIONS

### Central Detector region

The central detector is designed mainly to measure those final state particles from the hard collision between the electron and the parton in the ion (Particles of types 1 and 3 in Fig. 2) and is very much like the traditional collider detectors.

The longitudinal kinematics of DIS is shown in the left panel of Fig. 5. The basic kinematic variables of DIS are  $Q^2 = -q^2$ , the virtuality of the exchanged photon,  $x$ , the fraction of the longitudinal momentum carried by the struck parton, and  $y$ , the inelasticity of the collision. The three variables are related by  $Q^2 = sxy$ , where  $s$  is the cms energy of the

collision. Thus, measuring any two of  $x$ ,  $y$ , or  $Q^2$ , specifies the longitudinal kinematics of DIS completely. While this measurement of two variables (taken to be  $x$  and  $Q^2$ ) is not enough for much of the physics program at the EIC, they need to be measured for almost all events to be used for physics analyses.

The scattered electron energy  $E_e$  and the scattering angle  $\vartheta_e$  can be used to reconstruct the variables,  $x$  and  $Q^2$ . The angle of the scattered parton and its energy (substituted with the angle and energy of the associated jet,  $\vartheta_{jet}$  and  $E_{jet}$ ) can also be used. Conversely, specifying  $x$  and  $Q^2$  completely determines the four measurable variables,  $\vartheta_e$ ,  $\vartheta_{jet}$ ,  $E_e$  and  $E_{jet}$ . Therefore, the energy of the scattered electron or jet that point towards any particular region of the central detector (i.e. fixed  $\vartheta$ ) is predicted from simple kinematics and can be taken into account in detector design.

Access to the transverse kinematics (transverse momentum  $k_t$  and impact parameter  $b_t$ ), beyond  $x$  and  $Q^2$ , as well as flavor identification of the partonic collision is central to the nucleon and nuclear structure measurement program planned for the EIC (right panel of Fig.5). The energy scale of

	Electron-Endcap	Barrel	Hadron-Endcap
$E_e$	< 8 GeV	8 - 50 GeV	> 50 GeV
$E_{jet}$	< 10 GeV	10 - 50 GeV	20 - 100 GeV
$E, \text{ hadrons}$	< 10 GeV	< 15 GeV	15 - 50 GeV

Table 1.

transverse kinematics is in the order of  $\Lambda_{\text{QCD}}$  (~200 MeV). This means identification and precise measurements of single hadrons among the particles associated with the scattered partons (Particles of type 3 in Fig. 2) are needed. In order to determine the detector requirements, the momentum range of these particles in various parts of the central detector must be understood—this follows from understanding of the “jet” energy that is expected for a fixed  $\vartheta_{jet}$  and the momentum distribution of particles within that jet.

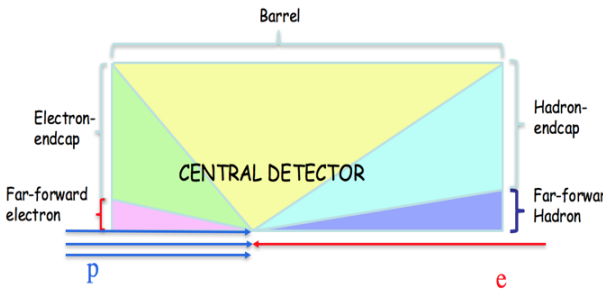


Figure 6: Regions in the JLEIC Central Detector.

The central detector is divided into three sections, the Electron-endcap, the Hadron-endcap and the Barrel as shown in Fig. 6. Far-forward sections (both electron and hadron) will be discussed separately. The three different central detector sections that correspond to different  $x$  and  $Q^2$  regions for the scattered electron are shown in the left panel of Fig. 7 along with the lines of constant scattered electron energy  $E_e$ . The same for the jet energies  $E_{jet}$  is shown in the right panel of Fig. 7.

From these figures, the range of energies for  $E_e$  and  $E_{jet}$  in each section of the detector can be read. Using Monte Carlo simulation the momentum range of hadrons that correspond to particles in each detector section can be estimated.

Table 1 gives, then, a rough estimate of the momenta for each of type of particle in each section.

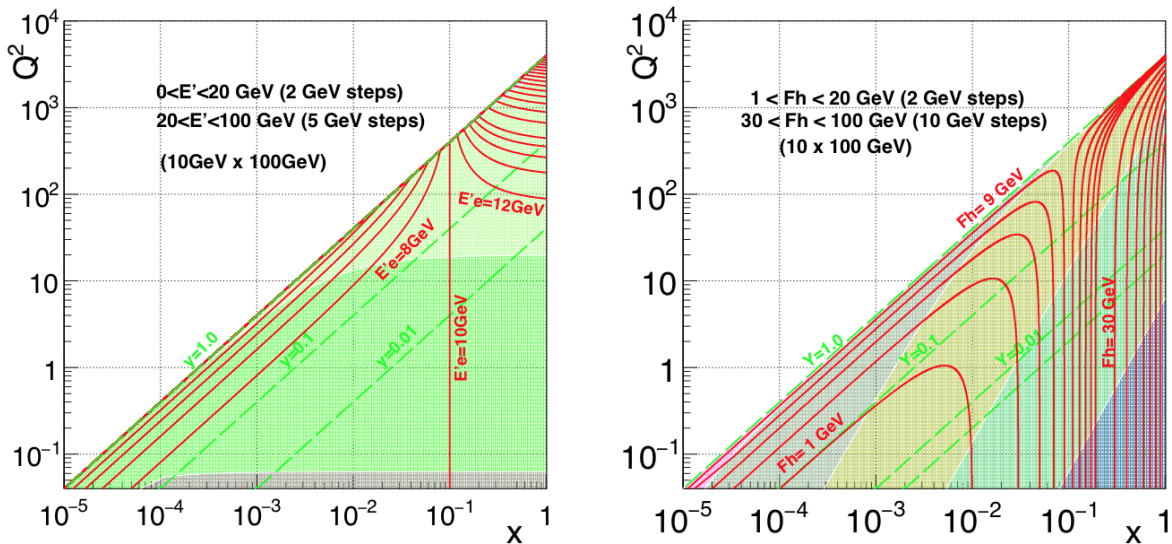


Figure 7: Isolines of the scattered electron (left panel) and jet (right panel) in the JLEIC Central Detector.

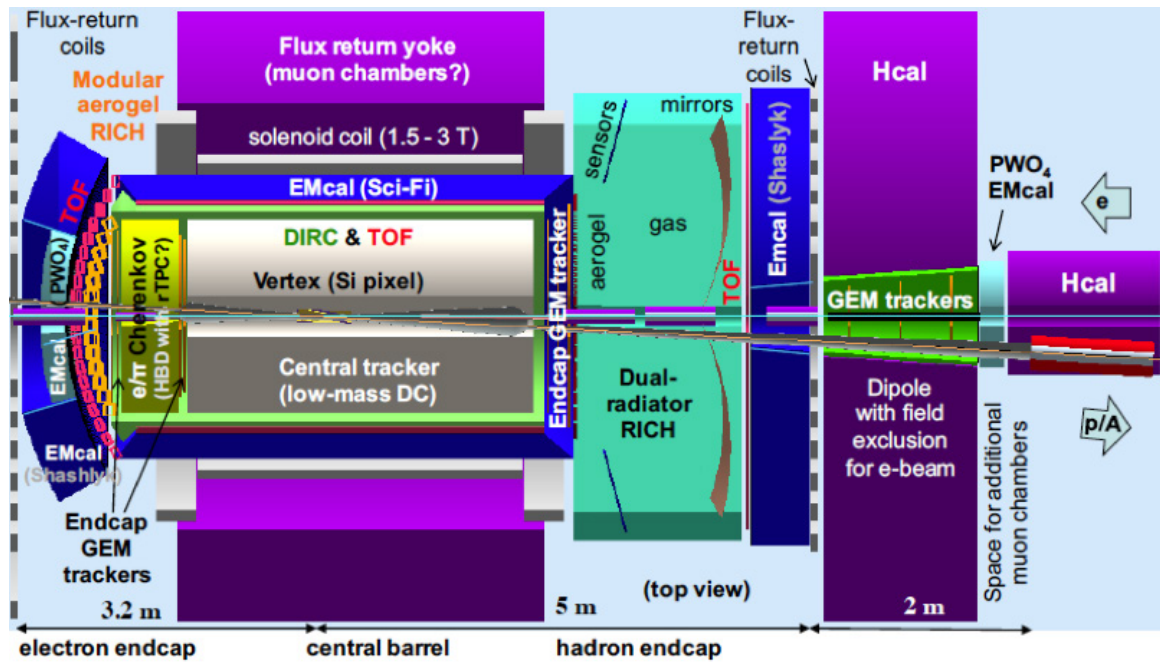


Figure 8: Detector concept for the JLEIC Central Detector

These energy ranges inform the choice of technologies needed in the central detector for tracking, calorimetry and particle identification. The current JLEIC central detector design is shown in Fig 8.

### Far-Forward hadron detector region

Crucial information on hadron structure is carried by particles that do not emerge from the beam envelope within the coverage of the central detector.

Broadly speaking, there are two types of forward final state particles that need to be reconstructed. The first type of forward particles comes from interactions in which the beam particle receives a large transverse momentum kick and fragment into many parts. These particles typically retain a velocity similar in magnitude, but significantly different kinematics from that of the beam particle, and may have very different charge-to-mass ratios. Such particles will separate relatively rapidly from the beam. An example of such a particle is a forward proton from a deuteron-electron DIS shown in Fig 9. Measurements of

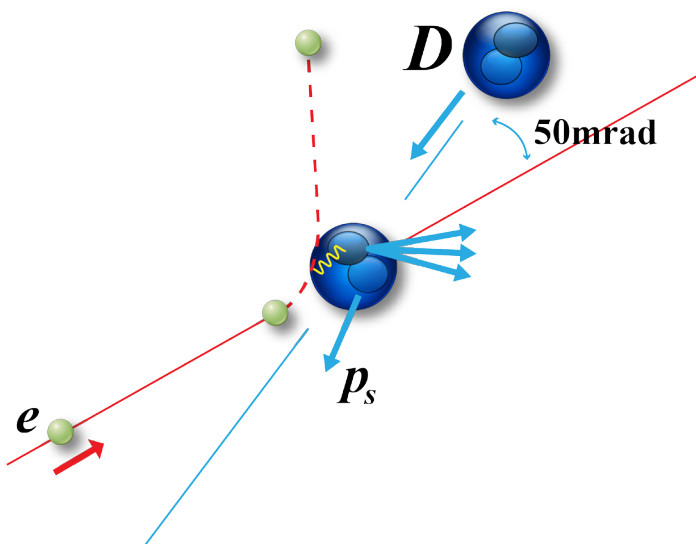


Figure 9: Electron-deuteron scattering at the JLEIC.

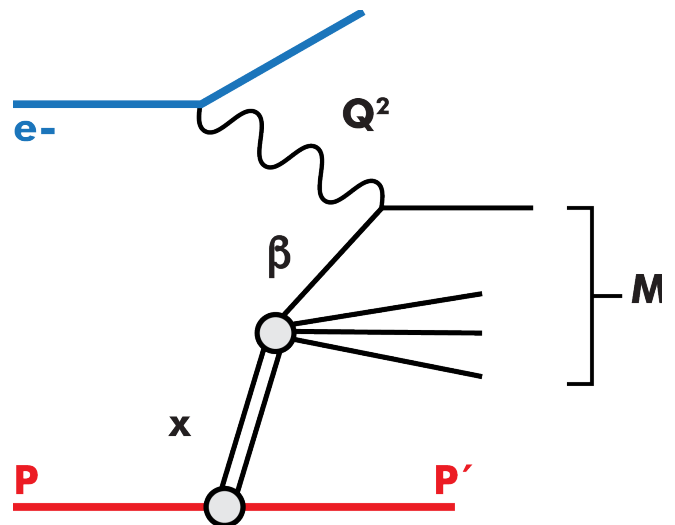


Figure 10: Illustration of a diffractive process.

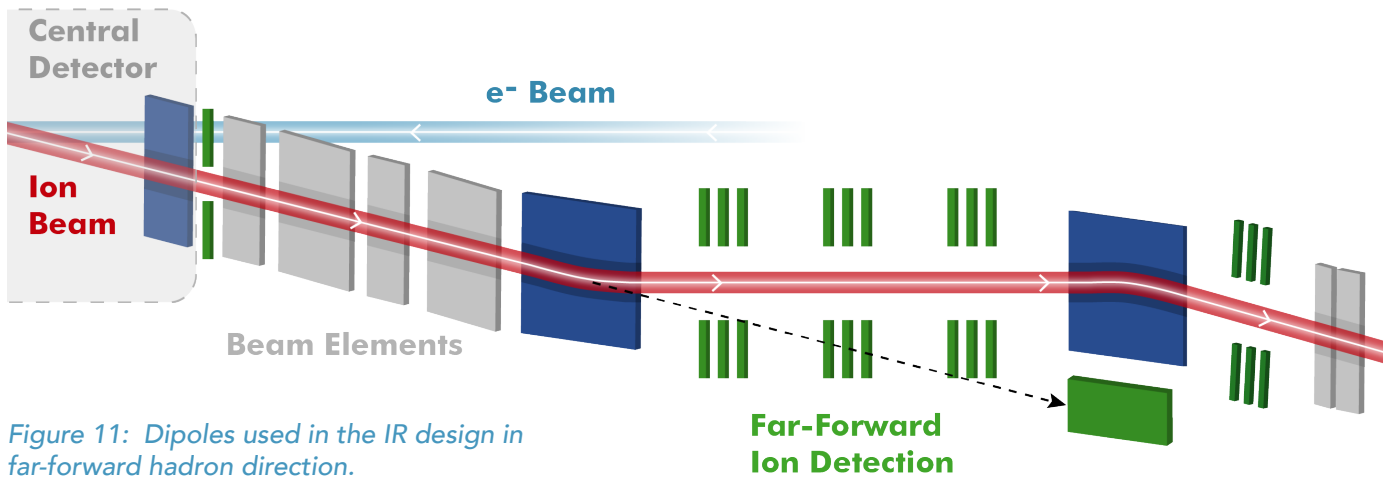


Figure 11: Dipoles used in the IR design in far-forward hadron direction.

such particles are important in understanding the nucleon-nucleon interactions in nuclei, as well as, in case of deuterons, determining the structure of neutrons.

The second type is the (hadron) beam particle that stays intact during the collision and only loses a small fraction of their momentum and acquires a small transverse momentum ( $p_T$ ). These particles are leading protons or ions in non-dissociative diffractive interactions (see Fig. 10), and will have a trajectory that is close to the proton (or the ion) beam.

There are two detector regions downstream of the ion beam after the central detector (see Fig. 11). The first area is between the first dipole downstream of the interaction point in the ion beam direction and the first ion FFQ; this region will be called the "first" forward detection region and is about 50 cm longitudinally. The first dipole provides about 1Tm of field integral and thus gives moderate analyzing power for those particles detected in the "first" forward region. After the FFQs, second and third, long dipoles (20Tm field integral each) provide the possibility of high-resolution measurements for those particles that pass through the apertures of the FFQs. The area, about 30m longitudinally, surrounding the two dipoles is the "second", or high-resolution, forward ion detection region. These two detector regions together with the detector systems in the central detector provide essentially 100% coverage

for final state particles associated with the incident ion (proton) beam particle.

The leading protons and ions in non-dissociative diffractive interactions, whose measurements are an important part of the EIC physics program, will be mainly measured in the high-resolution forward detector region. In order to maximize the acceptance and resolution for these particles, the optics of the beam is arranged such that there is a secondary focus of the beam at  $\sim 42\text{m}$  downstream of the interaction point. At the same point, the dispersion is designed to have a maximum. A detector system at this point will have maximum acceptance for final state particles whose momenta are close to that of the beam particles. Figure 12 shows the acceptance for protons generated at

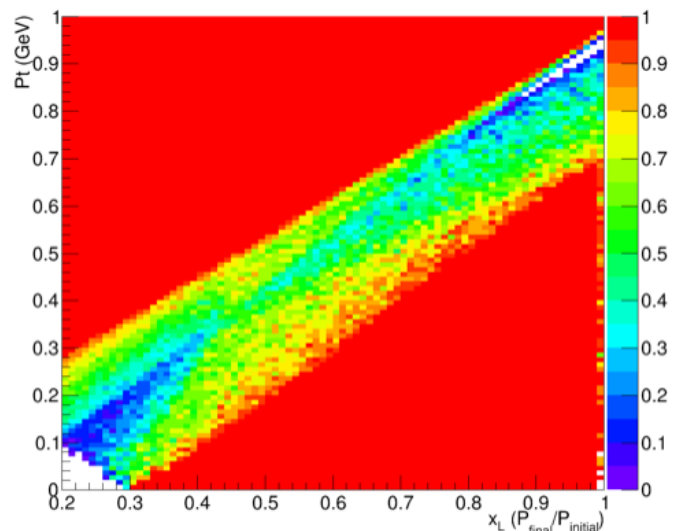


Figure 12: Simulated acceptance for far-forward protons from diffractive processes.

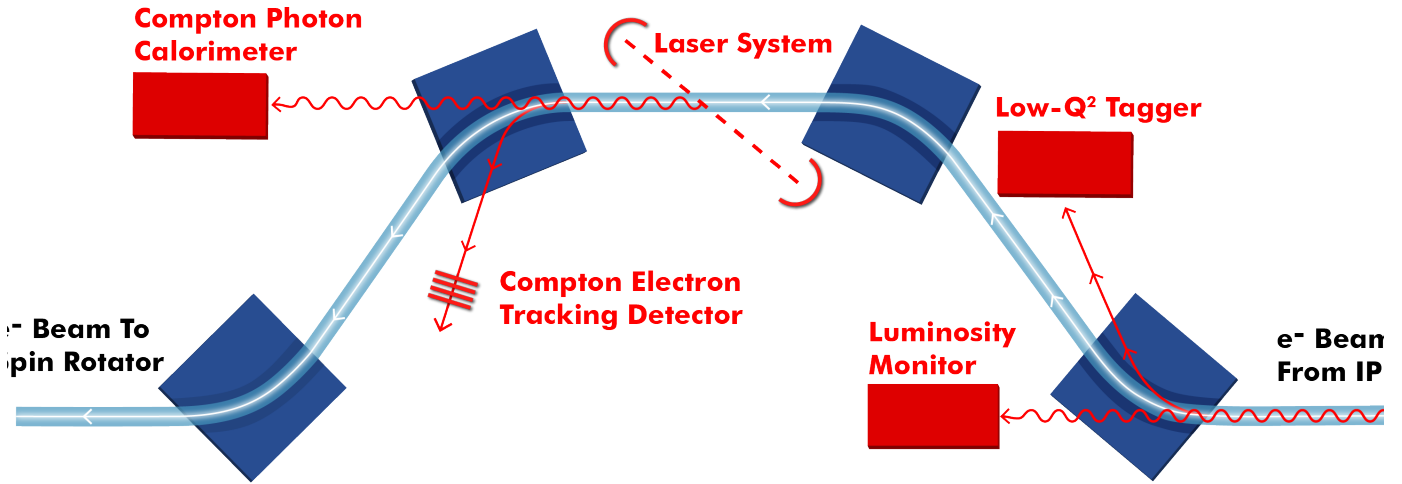


Figure 13: Illustration of the concept for detecting low Q2 events and measuring the polarization of the electron beam and the luminosity at the IP

the interaction point having energies of  $x_L \times 100$  GeV and having  $P_t$  up to 1 GeV. (i.e. momentum range expected for leading protons in non-dissociative interaction at a proton beam energy of 100 GeV). The acceptance is 100% in all of this area except for a diagonal region shadowed by the aperture of the FFQs. Even in this area, the acceptance is mostly above 50%. The lower right triangular area corresponds to the kinematics that will be measured in the high-resolution forward detection region. The large aperture of the FFQs also allows a large acceptance for zero-degree calorimeter placed at around 30 m downstream for neutron detection.

### Far-Forward Electron Detection region and ancillary measurements

Measurements of particles down to the beam-line in the electron-beam direction are also needed. The detector/IR design is expanded in the forward electron direction, as shown in Fig. 13 (see also Fig. 4) to monitor the luminosity and polarization of the electron-beam as well as to significantly increase the low-Q2 coverage of the detector.

Electron-ion scattering where the electron is scattered through a very shallow angle corresponds to the case where the exchanged photon is almost real. Such photoproduction processes are of interest in their own right; to characterize them, we would need to measure these electrons at shallow angles, which would be near the electron-beam.

The first dipole separates the electron beam from the particles that move close to the electron beam. It serves as an analyzing magnet for small-angle electrons and allows the reconstruction of the low Q2 events whose scattering electrons cannot be detected in the central detector. A detector for off-momentum electrons is placed after the first dipole as shown in Fig. 13.

The luminosity is measured via the Bethe-Heitler process. The same first dipole magnet separates the electron beam from the Bethe-Heitler photons that are travelling along the beam. This allows for luminosity measurement using a photon detector after the dipole as shown in Fig. 13.

Three dipole magnets are installed after the first dipole magnet, as shown in Fig. 13 to bring the electron beam back into the ring and

suppress the dispersion. This configuration is ideal for measuring the electron polarization, as shown in Fig. 13. The dipole magnets are identical, up to the direction of the field, so that their effects on the electron beam compensate each other. The polarization after the second dipole, up to the precision of the magnet parameters, is the polarization at the IP. This allows for measuring the beam polarization at a location of minimum background and with no space constraints. A laser system is installed in the straight section between the second and third dipole magnets. The third dipole magnet that bends the electron beam separates also the Compton photons from the Compton electrons. This allows for a combined analysis using both the Compton electrons and photons and will help to reduce the systematic uncertainties on the polarization measurement. The third dipole serves as an analyzing magnet for the Compton electrons. Because all dipoles in the chicane are identical, off momentum electrons that emerge from the central detector are constrained not to cross the beamline, and thus will not enter the Compton electron detector as background.

## Summary

The science program at the electron-ion collider (EIC) has the potential to revolutionize our understanding of nuclear and nucleon structure. It will also explore new states of QCD. In order to maximize the potential of an EIC, it is important to have a large (~100%) acceptance not only in the central region, but also in the region that is close to both the ion-beam and electron-beam direction—i.e. a total acceptance detector is needed. There has never been a collider detector that has both the central and forward acceptances that are near 100% and this design poses unique challenges.

This document briefly described the general drivers for the design and outlined some of the design elements that are currently being planned for the Jefferson Lab Electron-Ion Collider (JLEIC).

More technical information on the current design parameters are being continuously updated and can be found at <https://eic.jlab.org/wiki/>